Article

d Re-Based Olefin Metathesis Catalysts, Re(#CR)(CHR)(X)(Y): The Key Role of X and Y Ligands for Efficient Active Sites

Xavier Solans-Monfort, Eric Clot, Christophe Copret, and Odile Eisenstein

J. Am. Chem. Soc., **2005**, 127 (40), 14015-14025• DOI: 10.1021/ja053528i • Publication Date (Web): 15 September 2005

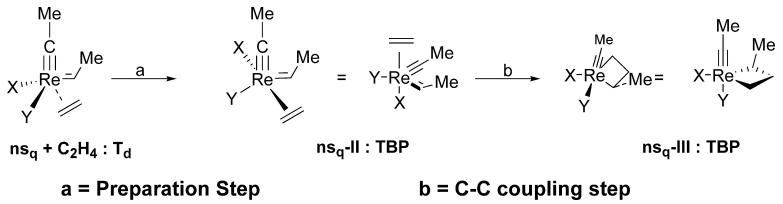

More About This Article

Additional resources and features associated with this article are available within the HTML version:

- Supporting Information
- Links to the 14 articles that cite this article, as of the time of this article download
- Access to high resolution figures
- Links to articles and content related to this article
- Copyright permission to reproduce figures and/or text from this article

View the Full Text HTML

J|A|C|S
ARTICLES
Published on Web 09/15/2005

d^0 Re-Based Olefin Metathesis Catalysts, Re(≡CR)(═CHR)(X)(Y): The Key Role of X and Y Ligands for Efficient Active Sites

Xavier Solans-Monfort,[†] Eric Clot,[†] Christophe Copéret,[‡] and Odile Eisenstein*,[†]

Contribution from LSDSMS (UMR 5636 CNRS), cc 14, Institut Gerhardt, Université Montpellier 2, F-34095 Montpellier Cedex 5, France, and LCOMS (UMR 9986 CNRS−CPE Lyon), 43 Boulevard du 11 Novembre 1918, F-69616 Villeurbanne Cedex, France

Received May 30, 2005; E-mail: odile.eisenstein@univ-montp2.fr

Abstract: DFT(B3PW91) calculations show that the reaction pathways for ethylene metathesis with Re(≡CMe)(═CHMe)(X)(Y) (X/Y = CH_2CH_3/CH_2CH_3; CH_2CH_3/$OSiH_3$; $OSiH_3$/CH_2CH_3; OCH_3/OCH_3, CH_2CH_3/OCH_3, and OCF_3/OCF_3) occur in two steps: first, the pseudo-tetrahedral d^0 Re complexes distort to a trigonal pyramid to open a coordination site for ethylene, which remains far from Re (early transition state for C−C bond formation). The energy barrier, determined by the energy required to distort the catalyst, is the lowest for unsymmetrical ligands (X ≠ Y) when the apical site of the TBP is occupied by a good σ-donor ligand (X) and the basal site by a poor σ-donor (Y). Second, the formation of metallacyclobutanes (late transition state for C−C bond formation) has a low energy barrier for any type of ligands, decreasing for poor σ-donor X and Y ligands, because they polarize the Re−C alkylidene bond as $Re^{+\delta}$═$C^{-\delta}$, which favors the reaction with ethylene, itself polarized by the metal center in the reverse way. The metallacyclobutane is also a TBP, with apical alkylidyne and Y ligands, and it is stabilized by poor σ-donor X and Y. The best catalyst will have the more shallow potential energy surface, and will thus be obtained for the unsymmetrical set of ligands with X = a good σ-donor (alkyl) and Y = a poor σ-donor (O-based ligand). This rationalizes the high efficiency of well-defined Re alkylidene supported on silica, compared to its homogeneous equivalent, Re(≡CMe)(═CHMe)$(OR)_2$.

Introduction

Transition-metal catalyzed olefin metathesis has had a tremendous impact on polymer chemistry, basic and fine chemicals synthesis.[1−7] Some very efficient catalysts have been discovered, but the detailed factors that increase their efficiency are not known. Therefore, catalyst design makes use only of very general principles. For example, the elementary steps of olefin metathesis are considered to be the coupling of the M═C and C═C bonds and the corresponding reverse reaction as proposed by Chauvin (Scheme 1).[8]

While the pathway proposed by Chauvin is universally accepted, olefin metathesis probably requires additional steps. For instance, in the case of the Grubbs' catalyst, $RuCl_2$(═CHR)-L_2 must lose a ligand to allow the approach of the olefin cis to the alkylidene group.[9] Similarly in the case of tetrahedral d^0 alkylidene complexes, the olefin must interact with the metal center, which is considered to be electron deficient (a Lewis acid center to attract the incoming olefin, a Lewis base). Most of the experimental facts support this hypothesis. Thus, the d^0 alkylidene imido complexes of group 6 metals (Mo and W), M(═NAr)(═CHR′)$(OR'')_2$ (see **A** below for a representative example)[1,6] are more efficient than group 7 (Re) alkylidyne complexes Re(≡C*t*Bu)(═CHR′)$(OR'')_2$ (see **B** for a representative example)[10−14] because of a combination of a more electropositive metal and a more electronegative ligand. Conversely, the increase of the catalytic activity with the electronegativity of the alkoxy substituents, e.g., R″ = $C(CH_3)(CF_3)_2$ > R″ = $C(CH_3)_3$ illustrates the same general principle.[14] The grafting of Re(≡C*t*Bu)(═CH*t*Bu)$(CH_2tBu)_2$ on silica to form the well-

Scheme 1. Chauvin Olefin Metathesis Mechanism

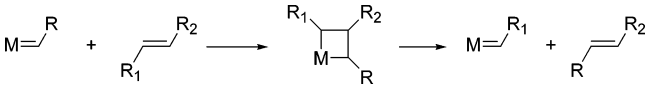

[†] LSDSMS.
[‡] LCOMS.

(1) Schrock, R. R. *J. Mol. Catal. A-Chem.* **2004**, *213*, 21.
(2) Grubbs, R. H.; Chang, S. *Tetrahedron* **1998**, *54*, 4413.
(3) Fürstner, A. *Angew. Chem., Int. Ed.* **2000**, *39*, 3012.
(4) Astruc, D. *New J. Chem.* **2005**, *29*, 42.
(5) Mol, J. C. *J. Mol. Catal. A-Chem.* **2004**, *213*, 39.
(6) Schrock, R. R. *Tetrahedron* **1999**, *55*, 8141.
(7) Trnka, T. M.; Grubbs, R. H. *Acc. Chem. Res.* **2001**, *34*, 18.
(8) Hérisson, J. L.; Chauvin, Y. *Makromol. Chem.* **1971**, *141*, 161.
(9) (a) Weskamp, T.; Kohl, F. J.; Hieringer, W.; Gleich, D.; Herrmann, W. A. *Angew. Chem., Int. Ed. Engl.* **1999**, *38*, 2416. (b) Vyboishchikov, S. F.; Bühl, M.; Thiel, W. *Chem. Eur. J.* **2002**, *8*, 3962.
(10) Toreki, R.; Schrock, R. R. *J. Am. Chem. Soc.* **1990**, *112*, 2448.
(11) Toreki, R.; Schrock, R. R.; Davis, W. M. *J. Am. Chem. Soc.* **1992**, *114*, 3367.
(12) Toreki, R.; Schrock, R. R.; Vale, M. G. *J. Am. Chem. Soc.* **1991**, *113*, 3610.
(13) Vaughan, G. A.; Toreki, R.; Schrock, R. R.; Davis, W. M. *J. Am. Chem. Soc.* **1993**, *115*, 2980.
(14) Toreki, R.; Vaughan, G. A.; Schrock, R. R.; Davis, W. M. *J. Am. Chem. Soc.* **1993**, *115*, 127.

10.1021/ja053528i CCC: $30.25

defined Re(≡C*t*Bu)(=CH*t*Bu)(CH_2*t*Bu)(OSi≡) species, **C**,[15] provides a highly active catalyst, which becomes even more efficient than the most efficient molecular catalyst Re(≡CR)(=CHR′)(OC(CH_3)(CF_3)$_2$)$_2$.[16] Spectroscopic studies[17,18] have shown that the grafted species can be considered as a quasi-molecular complex, where the surface acts as a large siloxy ligand. Therefore, the major difference between these systems, Re(≡CR)(=CHR′)(X)(Y), is the presence of equivalent X and Y ligands in the molecular system and different ones in the grafted system (X = CH_2*t*Bu and Y = OSi≡), and this suggests that other factors than the electrophilicity at the metal center might play a role on the global reaction rate.

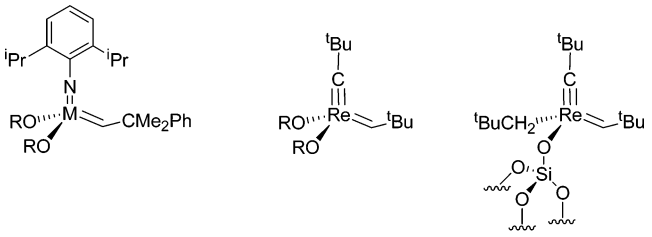

A **B** **C**

The Chauvin mechanism[4,8] implies that the olefin comes in close vicinity of the M=CHR bond to form the metallacyclobutane, and this is facilitated when a low lying empty metal orbital is available (an electrophilic metal center). However, such a low lying orbital is absent in a tetrahedral complex. Thus, it is necessary to analyze how the nature of the ligands contributes to the ability of the metal fragment to generate the proper orbital pattern to prepare the catalyst to carry out the [2+2] cycloaddition. A better understanding of this aspect has many implications on the specificity and the efficiency of the reaction.

Computational studies on the reactivity of metathesis reaction have been carried out. Most of the efforts have been concentrated on the Ru-carbene catalysts.[9,19] In the case of d^0 Mo imido complexes, computational studies have been focused on the electronic structure of the starting alkylidenes[20,21] and the molybdacyclobutane intermediates.[22−25] Wu and Peng have computed the reaction pathways for olefin metathesis of Mo(=NH)(=CHR)(OR′)$_2$ (R = H, Me, R′ = CH_3, CF_3) with C_2H_4 at the B3LYP level, confirming the increased reactivity with the more electron-withdrawing groups OCF_3.[26] Recently, the same authors have presented a theoretical study of the reaction of Mo(=NH)(=CH_2)(OR)$_2$ (R = CH_3, CF_3) with norbornadiene.[27] In an even more recent paper, the factors affecting chiral recognition to the observed products have been studied for the asymmetric Mo(=NR)(=CHR′)(OR″)(OR‴) catalyst.[28] The reactivity of Mo-oxo alkylidene complexes grafted on alumina has been studied with a cluster model of the surface.[29] In all molecular systems, that have been studied, the formation of the metallacycle occurs in a single step reaction, but the nature of the transition state has been found to vary greatly from very early[22,28] to very late,[26] without apparent reason since in particular the species studied by Lammertsma and Wu are similar.

In this work, we have carried out a computational study by DFT calculations of the metathesis of ethylene and Re(≡CCH_3)(=CHCH_3)(CH_2CH_3)$_2$ (**1**$_q$), Re(≡CCH_3)(=CHCH_3)(CH_2CH_3)(OR) (R = SiH_3, **2**$_q$; R = CH_3, **2**$_q$**-OMe**) and Re(≡CCH_3)(=CHCH_3)(OR)$_2$ (R= CH_3, **3q**; R = CF_3, **3**$_q$**-OCF**$_3$). Our goal is to understand the electronic criteria, favoring the coordination of the olefin and the formation of the metallacyclobutane. This work reveals the existence of a key step apart from the [2+2] cycloaddition, during which the catalyst is prepared via the generation of a coordination site on the metal. The electronic requirements for the two steps are different and rationalize the effects of ancillary ligands on the efficiency of the catalysts, thus providing an interpretation for the efficiency of the silica supported complex.

Computational Details

Calculations have been carried out with the hybrid B3PW91 density functional,[30,31] as implemented in the Gaussian98 package[32] on the model systems Re(≡CCH_3)(=CHCH_3)(X)(Y) (X = Y = CH_2CH_3 for **1**$_q$; X = CH_2CH_3, Y = $OSiH_3$ for **2**$_q$; X = CH_2CH_3, Y = OCH_3 for **2**$_q$**-OMe**; X = Y = OCH_3 for **3**$_q$; X = Y = OCF_3 for **3**$_q$**-OCF**$_3$) reacting with ethylene (eq 1). The Re and Si atoms have been represented with the quasi relativistic effective core pseudo-potentials (RECP) of the Stuttgart group and the associated basis sets augmented with a polarization function (Re: α = 0.869; Si: α = 0.284).[33,34] The remaining atoms (C, H, O, and F) have been represented with 6-31G(d,p) basis sets.[35] The B3PW91 geometry optimizations were performed without any symmetry constraints, and the nature of the extrema (local minima or transition states) was checked by analytical frequency calculations. The energies given throughout the paper are electronic energies *E* without any ZPE corrections (inclusion of the ZPE corrections does not significantly modify the results) or Gibbs free energy values *G* computed with Gaussian 98 at 298 K and *P* = 1 atm. The atomic charges have been calculated using the Natural Population Analysis (NPA) scheme of Weinhold and co-workers.[36]

(15) Chabanas, M.; Baudouin, A.; Copéret, C.; Basset, J.-M. *J. Am. Chem. Soc.* **2001**, *123*, 2062.
(16) (a) Chabanas, M.; Copéret, C.; Basset, J.-M. *Chem. Eur. J.* **2003**, *9*, 971. (b) Copéret, C. *New J. Chem.* **2004**, *28*, 1.
(17) Chabanas, M.; Baudouin, A.; Copéret, C.; Basset, J.-M.; Lukens, W.; Lesage, A.; Hediger, S.; Emsley, L. *J. Am. Chem. Soc.* **2003**, *125*, 492.
(18) Copéret, C.; Chabanas, M.; Petroff Saint-Arroman, R.; Basset, J.-M. *Angew. Chem., Int. Ed.* **2003**, *42*, 156.
(19) (a) Aagaard, O. M.; Meier, R. J.; Buda, F. *J. Am. Chem. Soc.* **1998**, *120*, 7174. (b) Adlhart, C.; Hinderling, C.; Baumann, H.; Chen, P. *J. Am. Chem. Soc.* **2000**, *122*, 8204. (c) Adlhart, C.; Chen, P. *Angew. Chem., Int. Ed.* **2002**, *41*, 4484. (d) Adlhart, C.; Chen, P. *J. Am. Chem. Soc.* **2004**, *126*, 3496. (e) Fomine, S.; Martinez Vargas, S.; Tlenkopatchev, M. A. *Organometallics* **2003**, *22*, 93. (f) Cavallo, L. *J. Am. Chem. Soc.* **2002**, *124*, 8965. (g) Suresh, C. H.; Koga, N. *Organometallics* **2004**, *23*, 76. (h) van Speybroeck, V.; Meier, R. J. *Chem Soc. Rev.* **2003**, *32*, 151. (i) Burdett, K. A.; Harris, L. D.; Margl, P.; Maughon, B. R.; Mokhtar-Zadeh, T.; Saucier, P. C.; Wasserman, E. P. *Organometallics* **2004**, *23*, 2027.
(20) Cundari, T. R.; Gordon, M. S. *Organometallics* **1992**, *11*, 55.
(21) Fox, H. H.; Schofield, M. H.; Schrock, R. R. *Organometallics* **1994**, *13*, 2804.
(22) Folga, E.; Ziegler, T. *Organometallics* **1993**, *12*, 325.
(23) (a) Rappé, A. K.; Goddard, W. A., III *J. Am. Chem. Soc.* **1980**, *102*, 5114. (b) Rappé, A. K.; Goddard, W. A., III *J. Am. Chem. Soc.* **1982**, *104*, 448.
(24) Monteyne, K.; Ziegler, T. *Organometallics* **1998**, *17*, 5901.
(25) Sodupe, M.; Lluch, J. M.; Oliva, A.; Bertran, J. *New J. Chem.* **1991**, *15*, 321.
(26) Wu, Y.-D.; Peng, Z.-H. *J. Am. Chem. Soc.* **1997**, *119*, 8043.
(27) Wu, Y.-D.; Peng, Z.-H. *Inorg. Chim. Acta* **2003**, *345*, 241.
(28) Goumans, T. P. M.; Ehlers, A. W.; Lammertsma, K. *Organometallics* **2005**, *24*, 3200.
(29) (a) Handzlik, J.; Ogonowski, J. *J. Mol. Catal. A-Chem.* **2001**, *175*, 215. (b) Handzlik, J.; Ogonowski, J. *J. Mol. Catal. A-Chem.* **2002**, *184*, 371. (c) Handzlik, J. *J. Catal.* **2003**, *220*, 23. (d) Handzlik, J. *J. Mol. Catal. A-Chem.* **2004**, *218*, 91. (e) Handzlik, J. *Surf. Sci.* **2004**, *562*, 101.
(30) Becke, A. D. *J. Chem. Phys.* **1993**, *98*, 5648.
(31) Perdew, J. P.; Wang, Y. *Phys. Rev. B* **1992**, *45*, 13244.
(32) Pople, J. A.; et al. *Gaussian 98*; Gaussian, Inc.: Pittsburgh, PA, 1998.
(33) Andrae, D.; Häussermann, U.; Dolg, M.; Stoll, H.; Preuss, H. *Theor. Chim. Acta* **1990**, *77*, 123.
(34) Bergner, A.; Dolg, M.; Küchle, W.; Stoll, H.; Preuss, H. *Mol. Phys.* **1993**, *80*, 1431.
(35) Hehre, W. J.; Ditchfield, R.; Pople, J. A. *J. Chem. Phys.* **1972**, *56*, 2257.
(36) Reed, A. E.; Curtiss, L. A.; Weinhold, F. *Chem. Rev.* **1988**, *88*, 899.

Scheme 2

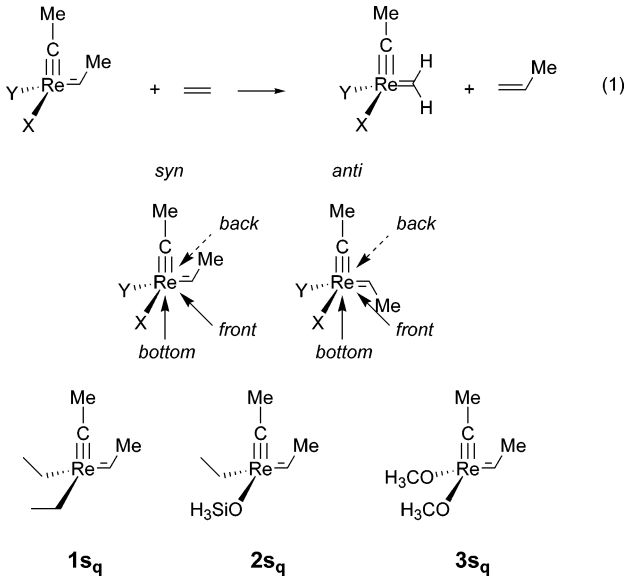

1s$_q$ **2s$_q$** **3s$_q$**

Results

DFT calculations for **1$_q$**, **2$_q$**, and **3$_q$** show that the alkylidene and alkylidyne groups are coplanar leading to syn- and anti-rotamers of similar energy.[37] In olefin metathesis, the alkene can potentially approach cis to the alkylidene ligand from three (*front*, *back*, and *bottom*) of the four triangular faces of the tetrahedron (Scheme 2). Note that the *bottom* approach requires rotation of the alkylidene group, in contrast to the approach to the two other faces, which are inequivalent only in the case of **2$_q$**. We have therefore studied the reaction pathways for ethylene with the two rotamers of the catalysts, **1s$_q$** and **1a$_q$**, for *front* and *bottom* approaches (the *bottom* approach is identical for both isomers). These calculations show that the *bottom* approach is energetically unfavorable and only the *front (back)* approach is possible. They also show that the reactivity of the anti isomer differs only slightly from that of the syn isomer. Because we focus on the effect of X and Y, we have thus only considered the reaction with the syn isomers in the case of complexes **2$_q$** (*front* and *back* approaches) and **3$_q$** (*front* approach).

Bis-alkyl Complex Re(≡CCH$_3$)(=CHCH$_3$)(CH$_2$CH$_3$)$_2$ (1s$_q$, 1a$_q$ and 1$_q$bottom). Front Approach to the syn Isomer 1s$_q$. The optimized geometries of the extrema located along the reaction pathway for the *front* approach are shown in Figure 1 and selected geometrical parameters are collected in Table 1. The relative energies (ΔE) and the Gibbs free energies (ΔG) values, evaluated from separated **1s$_q$** + C_2H_4, are given in Table 2 (*vide infra* for a comparison of the energy and free energy profiles for **1s$_q$**, **2s$_q$**, and **3s$_q$**).

The first step consists of the endothermic formation of the ethylene adduct **1s$_q$-II** (ΔE = 7.1 kcal mol^{-1}) via transition state **1s$_q$-TSI** lying 12.3 kcal mol^{-1} in energy above the separated reactants. The ethylene adduct **1s$_q$-II** has a trigonal bipyramidal (TBP) geometry with apical C_2H_4 and ethyl groups (X), and the alkylidene, alkylidyne and ethyl (Y) groups in the equatorial plane. The sum $\Sigma\alpha$ of the angles between the equatorial ligands (C(1)−Re−C(2), C(1)−Re−C(3), and C(2)−Re−C(3)) is equal to 359.9° showing that these ligands are coplanar. Ethylene is weakly bonded to the metal as illustrated by the long Re−C(5) and Re−C(6) distances of 2.461 and 2.446 Å, respectively and is staggered with respect to the alkylidyne and alkylidene ligands (as shown by the dihedral angle δ = C(2)−Re−C(6)−C(5) in Table 1). The main ethylene−Re interaction comes from the donation of the π ethylene orbital to the LUMO of the trigonal pyramid fragment, but this interaction does not provide any orientational preference. The orientation results from an interaction involving the ethylene π^* orbital. The metal is formally a d^0 center that cannot back-

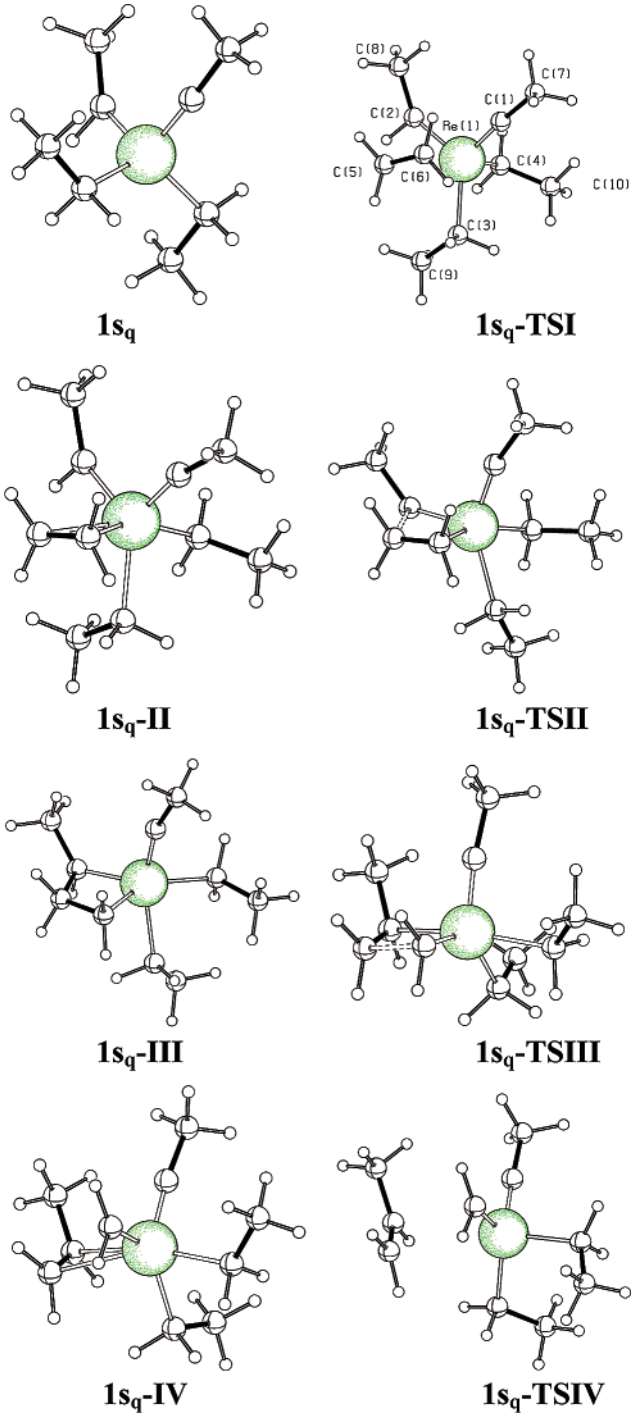

Figure 1. B3PW91 optimized geometries of the extrema located along the reaction pathway for the metathesis of ethylene with Re(≡CCH$_3$)(=CHCH$_3$)(CH$_2$CH$_3$)$_2$, **1s$_q$**. The numbering scheme used in the text is shown for **1s$_q$-TSI**.

(37) Solans-Monfort, X.; Clot, E.; Copéret, C.; Eisenstein, O. *Organometallics* **2005**, *24*, 1586.

Table 1. Selected Geometrical Parameters (distances in Å, angles in degrees) for the Extrema Located along the Metathesis Pathway of C_2H_4 with *syn*-Re(≡CCH_3)(=$CHCH_3$)(CH_2CH_3)$_2$ (**1s$_q$**)[a]

	1s$_q$-I	1s$_q$-TSI	1s$_q$-II	1s$_q$-TSII	1s$_q$-III	1s$_q$-TSIII	1s$_q$-IV	1s$_q$-TSIV
Re−C(1)	1.726	1.735	1.757	1.752	1.773	1.733	1.735	1.728
Re−C(2)	1.860	1.885	1.894	1.915	2.013	2.355	2.575	3.186
Re−C(3)	2.115	2.187	2.216	2.239	2.241	2.230	2.230	2.190
Re−C(4)	2.119	2.113	2.164	2.156	2.144	2.146	2.138	2.106
Re−C(5)		3.088	2.461	2.443	2.364	2.449	2.475	3.005
Re−C(6)		3.089	2.446	2.312	2.069	1.932	1.911	1.898
C(5)−C(2)		3.197	2.936	2.411	1.622	1.403	1.369	1.345
C(6)−C(1)		3.106	2.719	2.872	2.772	2.854	2.821	2.829
C(2)−C(1)	2.778	2.822	2.823	2.844	2.937	2.993	2.970	3.309
C(5)−C(6)		1.340	1.372	1.399	1.567	2.371	2.897	3.137
C(1)−Re−C(2)	101.5	102.3	101.2	101.7	101.6			
C(3)−Re−C(4)	122.0	98.0	81.3	83.6	82.9	79.1	80.8	78.5
C(1)−Re−C(3)	107.0	121.4	131.5	136.1	153.8	123.6	120.7	117.0
C(1)−Re−C(4)	106.9	98.8	95.6	93.4	90.0	94.6	97.1	97.7
Σα	317.5	353.7	359.9	359.3	357.3			
δ		51.1	42.9	10.3	2.2	−9.0	−37.4	−55.2

[a] The numbering scheme is shown in **1s$_q$-TSI** of Figure 1. Σα = C(1)−Re−C(2) + C(1)−Re−C(3) + C(2)−Re−C(3). δ = C(2)−Re−C(6)−C(5) up to **1s$_q$-III** and C(6)−Re−C(2)−C(5) after metathesis.

Table 2. Electronic Energy *E* and Gibbs Free Energy *G* (in kcal mol^{-1}) for the Extrema[a] Located along the Metathesis Pathways with Re(≡CCH_3)(=$CHCH_3$)(CH_2CH_3)$_2$ (syn **1s$_q$** and anti **1a$_q$**), Re(≡CCH_3)(=$CHCH_3$)(CH_2CH_3)($OSiH_3$) (**2s$_q$**), Re(≡CCH_3)(=$CHCH_3$)(CH_2CH_3)(OCH_3) (**2s$_q$-OMe**), Re(≡CCH_3)(=$CHCH_3$)(CH_2CH_3)(OCH_3) (**3s$_q$**), and Re(≡CCH_3)(=$CHCH_3$)(CH_2CH_3)(OCF_3) (**3s$_q$-OCF$_3$**)

catalyst		extrema								
		I	TSI	II	TSII	III	TSIII	IV	TSIV	V
1s$_q$	Δ*E*	0.0	12.3	7.1	8.2	−1.0	9.4	7.9	11.9	−1.2
	Δ*G*	0.0	25.0	22.4	24.7	17.9	26.0	23.0	24.7	−1.3
1a$_q$	Δ*E*	2.2	13.6	8.7	9.0	0.2	[b]	10.3	12.0	−1.2
	Δ*G*	2.4	26.5	23.7	25.9	18.8	[b]	26.1	25.0	−1.3
2s$_q$	Δ*E*	0.0	2.9	−0.2	1.7	−12.6	5.6	1.8	2.8	−0.9
	Δ*G*	0.0	13.1	13.7	17.4	4.2	21.7	15.6	15.4	−0.7
2s$_q$-OMe	Δ*E*	0.0	4.4	1.4	3.7	−9.6	7.3	3.2	4.1	−1.2
	Δ*G*	0.0	16.5	16.1	20.6	8.2	24.0	18.1	17.5	−0.2
3s$_q$	Δ*E*	0.0	9.3	−1.2	[b]	−15.2	2.7	2.3	8.7	−1.7
	Δ*G*	0.0	21.8	14.3	[b]	2.8	19.7	18.5	21.4	−1.3
3s$_q$-OCF$_3$	Δ*E*	0.0	6.3	[b]	[b]	−23.7	[b]	−3.7	7.7	0.6
	Δ*G*	0.0	19.0	[b]	[b]	−4.3	[b]	12.1	20.8	1.9

[a] **I** refers to the starting reactants Re(≡CCH_3)(=$CHCH_3$)(X)(Y) + C_2H_4, and **V** refers to the products Re(≡CCH_3)(=CH_2)(X)(Y) + C_3H_6. [b] Not located.

Scheme 3

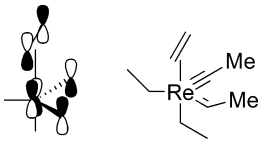

donate electron into the ethylene π* orbital. However, the formation of the Re−alkylidyne and Re−alkylidene multiple bonds leads to a partial occupancy of a Re d orbital of appropriate symmetry (left AA orbital in Figure 8 of ref 37), which in turn gives rise to a weak back-donation into π* of C_2H_4 optimized in the staggered orientation (Scheme 3). The donation and back-donation are small, and the C(5)−C(6) bond is only slightly elongated (1.372 Å in **1s$_q$-II** vs 1.330 Å in free ethylene).

The transition state **1s$_q$-TSI** has most of the features of intermediate **1s$_q$-II** but with the entering ethylene even further away from Re (Re···C(5) = 3.088 and Re···C(6) = 3.089 Å). For this reason, the alkylidyne, the alkylidene and alkyl ligands, which will be the equatorial ligands of the trigonal bipyramidal

Scheme 4. Schematic Geometrical Transformations Associated with the Approach of Ethylene and the Formation of the Metallacyclobutane

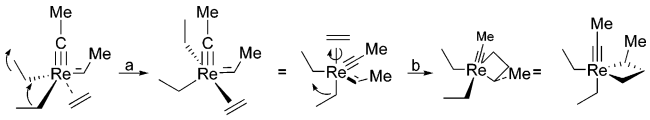

1s$_q$ + C_2H_4 : T_d **1s$_q$-II** : TBP **1s$_q$-III** : TBP

intermediate **1s$_q$-II**, are not yet coplanar (Σα = 353.7°). The increase in the Re−C bond lengths for the three ligands moving in the basal position is less than in **1s$_q$-II**. Upon going from **1s$_q$** to **1s$_q$-TSI** and finally to **1s$_q$-II**, the bond distances increase for Re−C(1) from 1.726, 1.735 to 1.757 Å, for Re−C(2) from 1.860, 1.885, to 1.894 Å and finally for Re−C(3) from 2.115, 2.187, to 2.216 Å. For the alkyl group going at the apical site, the Re−C(4) bond first shortens from 2.119 (**1s$_q$**) to 2.113 Å (**1s$_q$-TSI**) before lengthening to 2.164 Å in **1s$_q$-II** because of the stronger interaction with ethylene. At **1s$_q$-TSI**, the metal fragment is a trigonal pyramid with a far remote ethylene ligand. The transition state for the elementary step (**1s$_q$** + C_2H_4 to **1s$_q$-II**) describes thus a deformation of the tetrahedral reactant **1s$_q$**, which opens a coordination site to the incoming olefin. This occurs without yet any significant bonding with the entering ligand although the orientation of ethylene is already staggered with respect to the alkylidyne and alkylidene. It should be noted that the angle between the alkylidyne and the alkylidene ligands remains unchanged in the transformation between **1s$_q$** and **1s$_q$-II** (ca. 101°), suggesting that the Re−C multiple bonds are not affected. This transformation is thus best described as a motion of the two alkyl groups perpendicularly to the alkylidyne-Re-alkylidene plane, so that they occupy the apical and the equatorial sites of the trigonal bipyramid in **1s$_q$-II** (Scheme 4, step a). The energy barrier of 12.3 kcal mol^{-1} describes mostly the distortion of **1s$_q$** without any stabilization associated with the incoming ethylene.

The second step is the exothermic formation (Δ*E* = −8.1 kcal mol^{-1} relative to **1s$_q$-II**) of the rhenacyclobutane intermediate **1s$_q$-III** with a very low energy barrier of 1.1 kcal mol^{-1} via the transition state **1s$_q$-TSII**. The metallacyclobutane **1s$_q$-III** has a TBP geometry with axial alkylidyne and alkyl ligands. However, the angle between the alkylidyne and alkyl ligands,

C(1)−Re−C(3), is equal to 153.8° in place of 180° in an ideal TBP geometry because of their strong mutual trans effect. The geometry of the rhenacyclobutane is similar to those of other d^0 Mo or d^4 Ru metallacyclobutanes (see Table 1 for more details).[19g,26,28] The formation of the metallacyclobutane results from a [2+2] cycloaddition of the Re═CHMe and CH_2═CH_2 π-bonds. This allowed cycloaddition requires the olefin to rotate in order to eclipse the C═C bond with the Re-alkylidene bond (the dihedral angle C(2)−Re−C(6)−C(5) (δ) varies from 42.9° in **1s$_q$-II** to 10.3° in **1s$_q$-TSII**). The ethylene rotation is accompanied by an haptotropic shift of the ethylene from η^2 in **1s$_q$-II** to η^1 in **1s$_q$-TSII**, which significantly reduces the C(2)···C(5) distance (2.936 Å in **1s$_q$-II** and 2.411 Å in **1s$_q$-TSII**) and also, but in a much minor way, the Re−C(6) distance (2.446 Å in **1s$_q$-II** and 2.312 Å in **1s$_q$-TSII**). This shift polarizes the π system of the coordinated olefin to increase the negative charge on C_α and the positive charge on C_β.[38] This matches the electronic requirements of a metal-alkylidene bond polarized $Re^{+\delta}$═$C^{-\delta}$. The bond formation is accompanied by a reorientation of the ligands at Re. The alkyl group basal in **1s$_q$-II** becomes apical in the metallacyclobutane, and the distance between ethylene and the Re═CHMe moiety decreases (Scheme 4, step b). This geometry re-organization occurs without any significant energy barrier probably because of the very strong attractive interaction between the strongly polarized π-bonds.

From **1s$_q$-III** the reaction proceeds through the elementary steps that mirror those just described to form the final metathesis products, namely Re(≡CCH_3)(═CH_2)(CH_2CH_3)$_2$, **1$_q$-V**, and propene. The metallacycle **1s$_q$-III** decomposes through a [2+2] cycloreversion with a transition state **1s$_q$-TSIII** with a geometry similar to that of **1s$_q$-TSII** but lying 1.2 kcal mol^{-1} higher in energy (Table 2). The higher energy barrier associated with **1s$_q$-TSIII** is due to the cleavage of the two shorter bonds in the metallacyclobutane **1s$_q$-III** (C(6)−C(5) = 1.567 Å and Re−C(2) = 2.013 Å vs C(2)−C(5) = 1.622 Å and Re−C(6) = 2.069 Å) and the formation of the slightly less stable propene adduct **1s$_q$-IV** (0.8 kcal·mol^{-1} above **1s$_q$-II**). The geometry of the propene adduct is also a TBP with equatorial ethylidyne, methylene and ethyl groups. The geometries for the dissociation of propene through **1s$_q$-TSIV** is similar to that found for the coordination of ethylene in **1s$_q$-TSI** with a loosely bound axial olefin at more than 3 Å from Re in the trigonal bipyramidal complex, (CH_2═CHMe)Re(≡CCH_3)(═CH_2)(CH_2CH_3)$_2$ (Re−C(2) = 3.186 Å and Re−C(5) = 3.005 Å in **1s$_q$-TSIV**). An energy barrier of 4 kcal mol^{-1} is required for propene dissociation via **1s$_q$-TSIV** to form propene and the propagating methylene Re complex. As expected, the calculations found the overall reaction to be almost athermic.

Reaction with the anti Isomer 1a$_q$ and Bottom Approach. The geometries of the extrema located along the reaction pathway for ethylene metathesis with the anti isomer **1a$_q$** are shown in Figure S1 of the Supporting Information. All extrema are similar to that found for the syn isomer, and the energy barriers of all elementary steps are only slightly lower than for the syn isomer by an average of 1 kcal mol^{-1} (Table 2). The anti isomer is thus slightly more active than the syn isomer as observed experimentally by Schrock for the Mo-based complexes,[39] and computationally by Wu and Peng.[26] The difference in reactivity between the syn and anti rotamers is small, and the ligand effect on the reaction rate is probably more important. We have thus chosen to pursue the study of the reaction pathways for only one isomer since it is most likely that X and Y have similar influence on the reactivity of the two isomers. We have chosen to study the reactivity of the usually more abundant syn isomer.

When ethylene approaches along the *bottom* direction, the energy barrier for forming the ethylene adduct is 22.3 kcal mol^{-1} above the separated reactants (Figure S2). This is due to the mandatory rotation of the alkylidene ligand by 90°, which is energetically unfavorable and which rules out this reaction pathway.[37] In consideration of these results, the following studies on species **2$_q$** and **3$_q$** have been limited to the syn rotamers and the *front* (**3$_q$**) and *front* and *back* approaches (**2$_q$**).

Bis-Alkoxy Complex, Re(≡CCH_3)(═$CHCH_3$)(OCH_3)$_2$ (3s$_q$). The calculations have been performed for complexes with OCH_3 ligands as models for alkoxides. The geometries of the extrema along the metathesis reaction for **3s$_q$** and ethylene are represented in Figure 2, and selected geometrical parameters are given in Table S1 (see **3s$_q$-TSI** in Figure 2 for the atom labeling). The energy values are given in Table 2, and their graphical representation is shown in the discussion section.

Despite similar global geometrical features for the extrema, the energy profile is significantly different: all extrema are lower in energy relative to the entry point (**3s$_q$** + C_2H_4) than for the reference bis-alkyl system (**1s$_q$** + C_2H_4). The formation of **3s$_q$-II** is exothermic in contrast to being endothermic for **1s$_q$-II**, and the associated energy barrier is 3 kcal mol^{-1} lower. The formation of the rhenacyclobutane **3s$_q$-III** from **3s$_q$-II** is considerably more exothermic, ΔE (**3s$_q$-II** → **3s$_q$-III**) = −14.0 kcal mol^{-1}, than for the bis-alkyl system, ΔE(**1s$_q$-II** → **1s$_q$-III**) = −8.1 kcal mol^{-1}. Despite many attempts, the transition state for the [2+2] cycloaddition process, which should be similar to **1s$_q$-TSII**, could not be located. Because of the more exothermic reaction forming **3s$_q$-III**, the energy barrier is expected to be even lower than in the case of **1s$_q$** hence less than 1.1 kcal mol^{-1}. The decomposition of the metallacyclobutane occurs through the elementary steps (**3s$_q$-III** → **3s$_q$-IV** via **3s$_q$-TSIII**) and (**3s$_q$-IV** → metathesis products via **3s$_q$-TSIV**). The formation of the propene adduct **3s$_q$-IV** is endothermic (ΔE (**3s$_q$-III** → **3s$_q$-IV**) = 17.5 kcal mol^{-1}) with a very low energy barrier for back-reaction toward **3s$_q$-III** (ΔE (**3s$_q$-IV** → **3s$_q$-TSIII**) = 0.4 kcal mol^{-1}). This further confirms the very early nature of the transition state for the [2+2] cycloaddition (**3s$_q$-II** → **3s$_q$-III**), which could explain the difficulty to locate the associated transition state **3s$_q$-TSII**. The dissociation of propene from **3s$_q$-IV** is exothermic (ΔE between **3s$_q$-IV** and the metathesis products = −4.0 kcal mol^{-1}) with an energy barrier of 6.4 kcal mol^{-1} associated to the deformation of the TBP geometry of **3s$_q$-IV** toward the pseudo-tetrahedral geometry of Re(≡CCH_3)(═CH_2)(OCH_3)$_2$, **3$_q$-V**.

Mixed System Re(≡CCH_3)(═$CHCH_3$)($OSiH_3$)(CH_2CH_3) (2s$_q$). In the case of the complex with different X (CH_2CH_3) and Y ($OSiH_3$) ligands, the *front* (cis to the siloxy ligand) and *back* (trans to the siloxy ligand) approaches of ethylene leads to different reaction pathways. Remarkably, while the associated transition states, **2s$_q$-TSIfront** and **2s$_q$-TSIback**, have similar shapes, they have dramatically different energies above the entry point: 2.9 kcal mol^{-1} and 24.3 kcal mol^{-1} for **2s$_q$-TSIfront**

(38) (a) Eisenstein, O.; Hoffmann, R. *J. Am. Chem. Soc.* **1980**, *102*, 6148. (b) Eisenstein, O.; Hoffmann, R. *J. Am. Chem. Soc.* **1981**, *103*, 4308.
(39) Oskam, J. H.; Schrock, R. R. *J. Am. Chem. Soc.* **1993**, *115*, 11831.

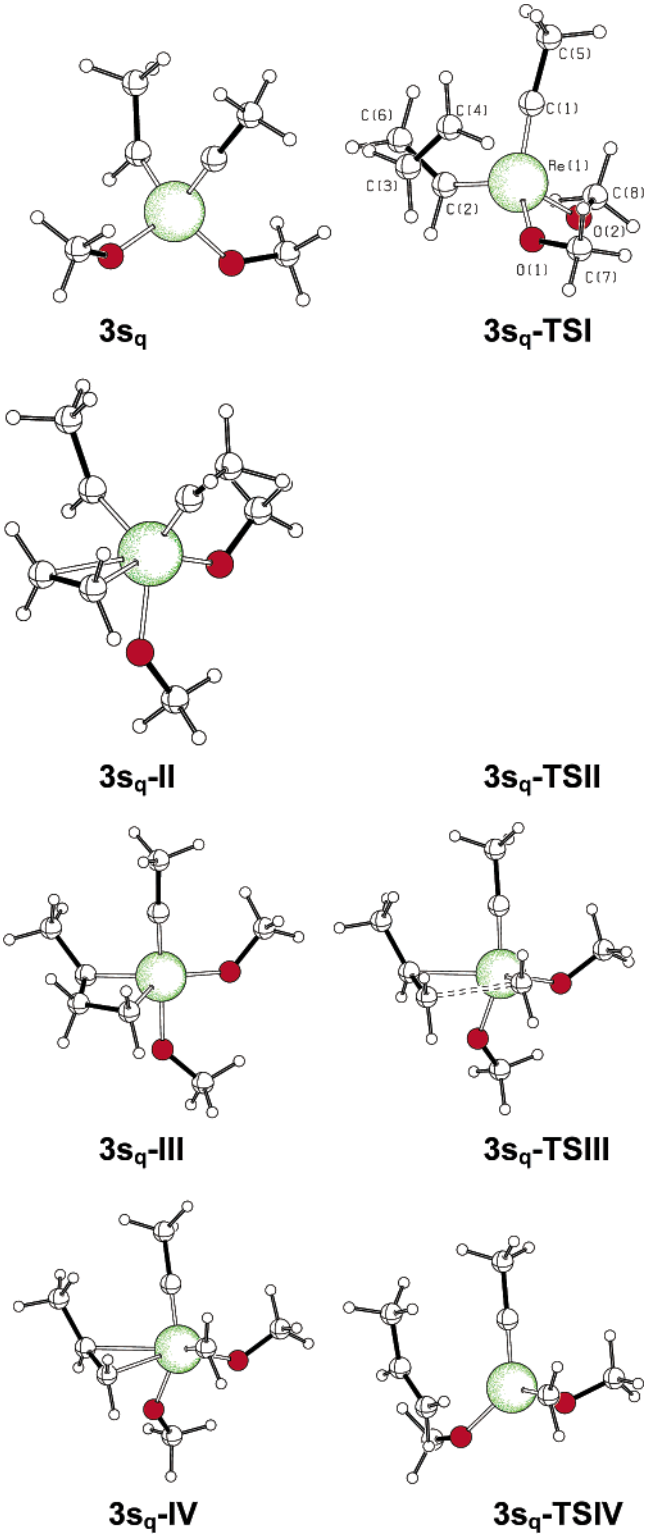

Figure 2. B3PW91 optimized geometries of the extrema located along the reaction pathway for the metathesis of ethylene with Re(≡CCH_3)-(═$CHCH_3$)(OCH_3)$_2$, **3s$_q$**. The TS structure **3s$_q$-TSII** could not be located (see text for details). The numbering scheme used in the text is shown on **3s$_q$-TSI**.

and **2s$_q$-TSIback**, respectively (Figure 3). This rules out a reaction path through a *back* attack (cis to the alkyl ligand), which has therefore not been studied further. As obtained for **1s$_q$** and **3s$_q$**, the two transition states **2s$_q$-TSIfront** and **2s$_q$-TSIback** have trigonal bipyramidal geometries with an apical

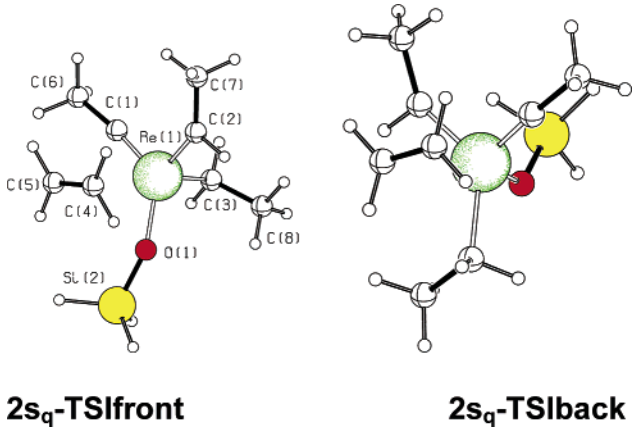

Figure 3. B3PW91 optimized geometries of the transition states for the formation of the ethylene adduct with axial ethyl (**2s$_q$-TSIfront**) or siloxy (**2s$_q$-TSIback**).

ethylene ligand. They only differ by the nature of the other apical ligand, the ethyl group for **2s$_q$-TSIfront** and the siloxy group for **2s$_q$-TSIback**. In the following, all extrema located on the pathway beyond **2s$_q$-TSI** have been obtained for the *front* attack and consequently the label *front* is limited to the transition state TSI and has been omitted for all other extrema for clarity in particular in Figures 4, 5, and 6.

The geometries of all extrema for the *front* attack are shown in Figure 4 (see **2s$_q$-TSIfront** for atom labeling) with selected geometrical parameters given in Table S2, and the energy values are given in Table 2 and graphically shown in the figures presented in the discussion. The ethylene adduct, **2s$_q$-II**, close in energy to the entry point is reached with a very low energy barrier. From this intermediate, the [2+2] addition occurs also with a very low energy barrier. The formation of metallacyclobutane is 12.6 kcal mol^{-1} exothermic relative to the entry point. The decomposition of the metallacyclobutane occurs via transition states that are slightly higher than for the formation of the metallacyclobutane, similarly to what was obtained for the other complexes.

Discussion

The energy and free energy profiles for the three pathways are shown in Figures 5 and 6, respectively. As expected from the loss of the relative translational component of the entropy in a bimolecular reaction, the Gibbs free energies (G) give higher barriers and less stable intermediates than suggested from the energy E. In particular, the metallacyclobutanes are no longer more stable than the separated reactants even with less bulky substituents than in the real systems. The entropy contribution destabilizes most the metallacyclobutanes and least the transition states for olefin addition, and it has an intermediate influence for the other extrema. The large decrease in the entropy component for the metallacyclobutane is associated with its relative rigidity and the smaller decrease in the entropy component for ***n*s$_q$-TSI** ($n = 1-3$) associated with a very weak interaction between the metal fragment and ethylene. The incorporation of the entropy disfavors more the steps where the metallacyclobutane is formed or cleaved (Scheme 4, step b) than those where the olefin approaches or leaves (Scheme 4, step a). However, it has been suggested that the entropic contribution may be exaggerated when calculated in gas phase from the harmonic approximation,[40] and the activation barriers may be

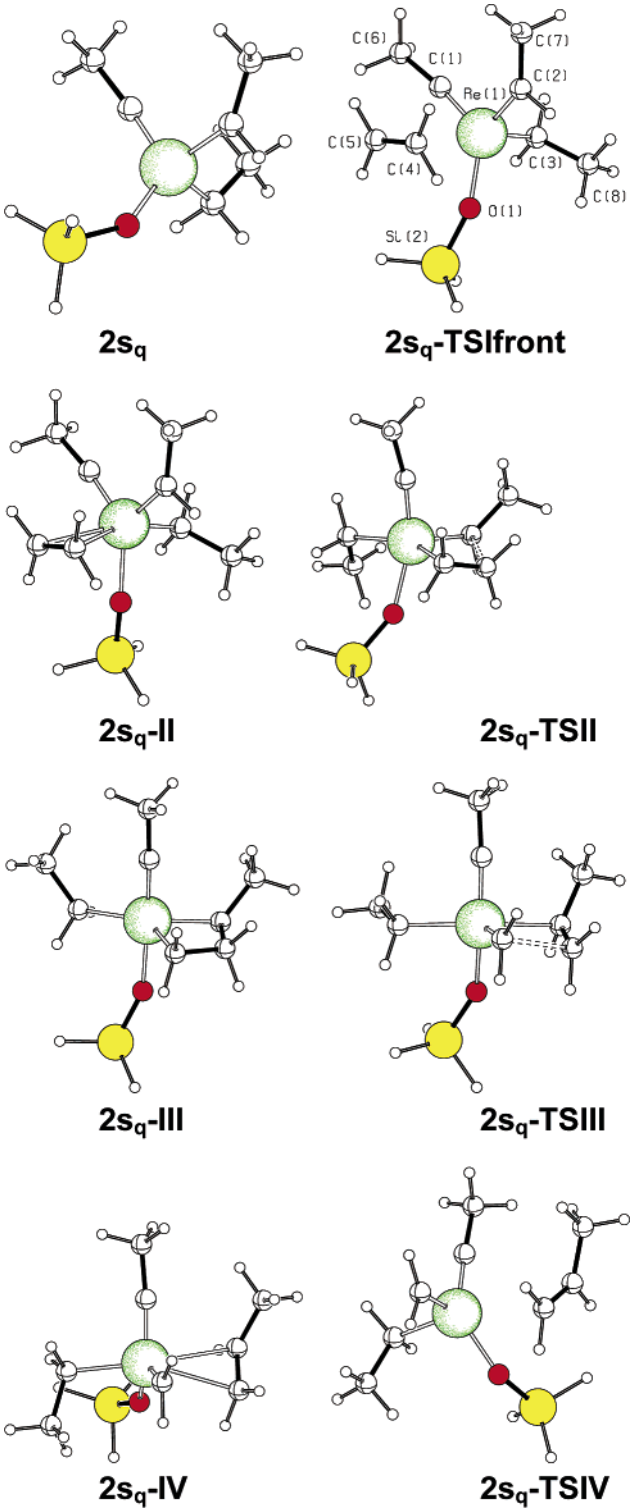

Figure 4. B3PW91 optimized geometries of the extrema located along the reaction pathway for the metathesis of ethylene with Re(≡CCH$_3$)(=CHCH$_3$)(OSiH$_3$)(CH$_2$CH$_3$), **2s$_q$** resulting from the front approach. The numbering scheme used in the text is shown in **2s$_q$-TSIfront**.

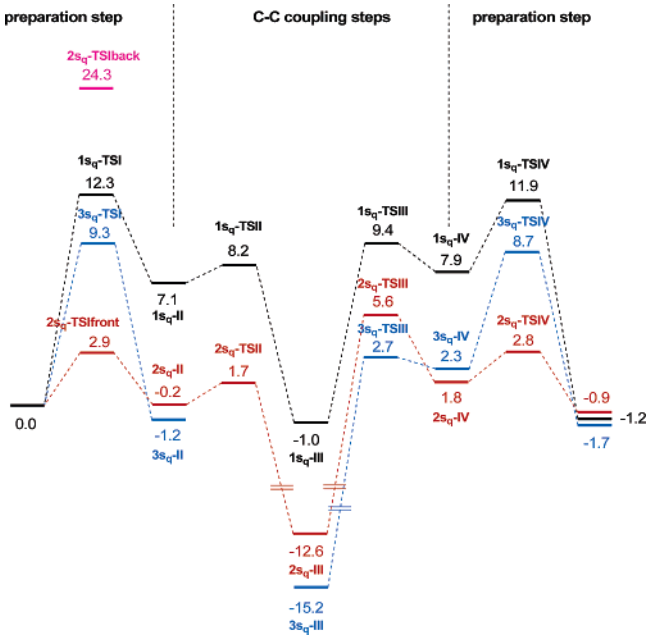

Figure 5. Comparison of the Potential Energy Surfaces (electronic energy E in kcal mol^{-1}) for the metathesis reaction of C_2H_4 with Re(≡CCH$_3$)(=CHCH$_3$)(X)(Y) (X = Y = CH$_2$CH$_3$, **1s$_q$**; X = CH$_2$CH$_3$, Y = OSiH$_3$, **2s$_q$**; X = Y = OCH$_3$, **3s$_q$**). For each systems the separated reactants **1s$_q$** + C_2H_4 (respectively **2s$_q$** + C_2H_4 and **3s$_q$** + C_2H_4) are taken as the energy origin. In the case of **2s$_q$**, only the *front* attack is considered.

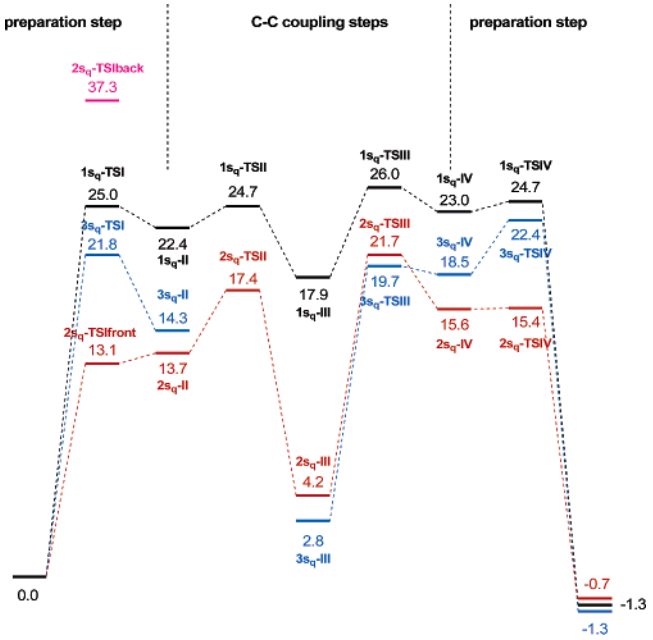

Figure 6. Comparison of the Gibbs free Energy Surfaces (Gibbs free energy G in kcal mol^{-1} at 298 K) for the metathesis reaction of C_2H_4 with Re(≡CCH$_3$)(=CHCH$_3$)(X)(Y) (X = Y = CH$_2$CH$_3$, **1s$_q$**; X = CH$_2$CH$_3$, Y = OSiH$_3$, **2s$_q$**; X = Y = OCH$_3$, **3s$_q$**). For each systems the separated reactants **1s$_q$** + C_2H_4 (respectively **2s$_q$** + C_2H_4 and **3s$_q$** + C_2H_4) are taken as the energy origin. In the case of **2s$_q$**, only the *front* attack is considered.

probably overestimated. The poor evaluation of entropy and the fact that the extrema are calculated from the potential energy surface *E* and not on the free energy surface *G* also result in some artifacts like the minimum **2s$_q$-II** having higher *G* values than the transition state **2s$_q$-TSIfront**. We thus prefer to discuss the reaction pathways on the basis of energies *E* than on Gibbs free energies *G*.

The reaction pathways for the olefin metathesis with these d^0 Re-based complexes are controlled by two individual steps, whose transition state energies depend strongly on X and Y,

(40) (a) Cooper, J.; Ziegler, T. *Inorg. Chem.* **2002**, *41*, 6614. (b) Sakaki, S.; Takayama, T.; Sumimoto, M.; Sugimoto, M. *J. Am. Chem. Soc.* **2004**, *126*, 3332. (c) Rotzinger, F. *Chem. Rev.* **2005**, *105*, 2003. (d) Leung, B. O.; Reidl, D. L.; Armstrong, D. A.; Rauk, A. *J. Phys. Chem. A* **2004**, *108*, 2720.

for both the formation (entry channel) and the decomposition (exit channel) of the metallacycle. The substituent pattern chosen in this study does not represent the one present in the full productive metathesis path since the alkylidene and olefin have been modeled, but each individual channel (coordination+[2+2] cycloaddition) illustrates the effect of ligands on the energy profile, and thus we discuss mostly the entry channel.

Coordinating Ethylene: Preparing the Catalyst. The theoretical literature has shown contradictory results for the transition state of olefin metathesis with d^0 tetrahedral alkylidene complexes. Ziegler has found an early transition state for the reaction with $MoCl_2(O)(=CH_2)$.[22] Moreover, while Wu and Peng have located a late transition state for $Mo(=NH)(=CH_2)(OR)_2$ (R = H, CH_3, CF_3),[26] Lammertsma et al. have found an early transition state in the case of $Mo(=NH)(=CH_2)(OCH_3)_2$.[28] The present work shows that the reaction of a d^0 tetrahedral $Re(\equiv CR)(=CHR)(X)(Y)$ complex with an olefin to form the metallacyclobutane occurs in two distinctive steps, leading to an early and a late transition states with respect to the carbon−carbon bond formation between the olefin and the alkylidene. The relative energies of these transition states are strongly influenced by the nature of the X and Y ligands.

The first transition state corresponds to the preparation of the catalyst. The rhenium center is surrounded by a total of 14 electrons when X = Y = CH_2CH_3, if the π bonds with the alkylidyne and alkylidene groups are included in the electron count. When X and/or Y have lone pairs (OR), it is usual to consider that the oxygen lone pair can be shared with the metal, which in principle should decrease the electron deficiency at the metal center although one should keep in mind that an O-based ligand is also a poor σ-donor ligand. This latter effect dominates, and the NBO charge at Re increases.[37] The metal being thus highly electron deficient in all cases, one should expect a high affinity for coordinating ethylene, leading to a low or no energy barrier for this step. The calculations show a more complex situation. A tetrahedral complex has no formal empty coordination site, and a structural change is mandatory to accommodate a fifth ligand. One coordination site is readily generated when the tetrahedron distorts into a trigonal prism, leading naturally to a trigonal bipyramid upon coordination of the olefin. Because the olefin must be cis to the alkylidene ligand and because the alkylidene and the alkylidyne must remain coplanar to keep the Re−C π-bonds, this imposes one of the ligand, X or Y, to go at the apical site of the TBP. The calculation shows that the first step describes such a structural change, and at the transition state (***n*s$_q$-TSI**, n = 1, 3) there is essentially no interaction with the incoming olefin. This corresponds to an early transition state with respect to the C−C bond formation between the olefin and the alkylidene. Moreover, the calculations show that the energy barrier is highly influenced by the nature of X and Y, and thus by the nature of the ligands going at the apical and basal sites respectively of the trigonal prism in the transition states ***n*s$_q$-TSI**.

The energy barrier associated with ***n*s$_q$-TSI** is the highest for X = $OSiH_3$ and Y = CH_2CH_3 (**2s$_q$-TSIback**, 24.3 kcal mol^{-1}). At much lower energies lies **1s$_q$-TSI** (X = Y = CH_2CH_3, 12.3 kcal mol^{-1}), followed by **3s$_q$-TSI** (X = Y = OCH_3, 9.3 kcal mol^{-1}) and finally the lowest transition state **2s$_q$-TSIfront** (X = CH_2CH_3 and Y = $OSiH_3$, 2.9 kcal mol^{-1}). Comparing the case (**1s$_q$**, X = Y = CH_2CH_3) to (**3s$_q$**, X = Y = OCH_3) shows that poorer σ-donor and better π-donor ligands slightly lower this transition state. Replacing the two OCH_3 by OCF_3 groups, to model the partially fluorinated alkoxide used experimentally, leads to even lower transition state (6.3 kcal mol^{-1} above the separated reactants). Therefore, introducing poorer and poorer electron donor ancillary ligands lowers the barrier of the first step of the reaction. It thus appears that the π-donating effect of the O-based ligand plays no stabilizing role because **TSI** has a lower energy for the poorer π-donor of the two alkoxy groups (OCF_3 vs OCH_3). This will appear to be the case in all situations, and we will retain the magnitude of the σ-donating group as a dominant electronic characteristic of X and Y in these complexes. Yet this analysis does not account for the situation corresponding to the lowest and the highest barriers. The lowest barrier is obtained for **2s$_q$-TSIfront** where the ethyl group, a good σ-donor, goes at the apical site and the siloxy group (poorer σ-donor) at the basal site. The highest barrier is obtained for **2s$_q$-TSIback** in which the sites occupied by the ethyl and siloxy groups have been exchanged. To check the specificity of a siloxy group as an O-based ligand, calculations have been carried out for **2s$_q$−OMe** (X = CH_2CH_3 and Y = OCH_3). The transition state has been found to be 4.4 kcal mol^{-1} above separated reactants, just slightly higher than for the siloxy group. Thus, for the step which corresponds to the coordination of the olefin, where the transition state is a trigonal pyramid metal fragment in very weak interaction with the olefin, the lowest barrier is associated with the apical and basal sites being occupied by a good σ-donor and a poor σ-donor, respectively (Scheme 6). More precisely, the effect of (X,Y) on the transition states is as follows. Comparing (CH_2CH_3, CH_2CH_3), (CH_2CH_3, OCH_3) and (CH_2CH_3, $OSiH_3$) shows that the barrier decreases when, for a given X, Y becomes a poorer σ-donor. Comparing ($OSiH_3$, CH_2CH_3) to (CH_2CH_3, CH_2CH_3) as well as (OCH_3, OCH_3) to (CH_2CH_3, OCH_3) shows that the barrier decreases when, for a given Y, X becomes a better σ-donor.

Scheme 5. Schematic Geometrical Transformations Associated with the Approach of Ethylene and the Formation of the Metallacyclobutane

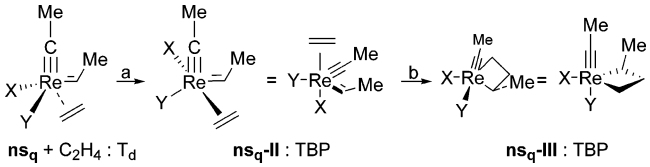

To understand the effect of ligands on the transition state energies, an energy partitioning scheme of the energy barrier ($\Delta E^{\ddagger}$) has been carried out (Table 3, eq 2). ΔE_{dis}(Re) and ΔE_{dis}(II) are the energies required to distort the catalyst and ethylene from the geometries they have as isolated entities to the ones they have as fragments in the transition states; ΔE_{int} is the interaction energy between the two fragments in the transition states (calculated as the difference between $\Delta E^{\ddagger}$ and the sum of ΔE_{dis}). The same partitioning analysis of the energy ΔE for **ns$_q$-II** has been carried out.

$$\Delta E^{\ddagger} = \Delta E_{dis}(\mathrm{Re}) + \Delta E_{dis}(\mathrm{II}) - \Delta E_{int} \qquad (2)$$

The results in Table 3 show that the energy barrier $\Delta E^{\ddagger}$ is essentially equal to the energy ΔE_{dis}(Re) required for distorting the metal fragment, all other contributions being very small and

Scheme 6. Energy (kcal mol^{-1}) of Transition States for Coordinating Ethylene to Re(≡CR)(=CHR)(X)(Y) with R = CH_3

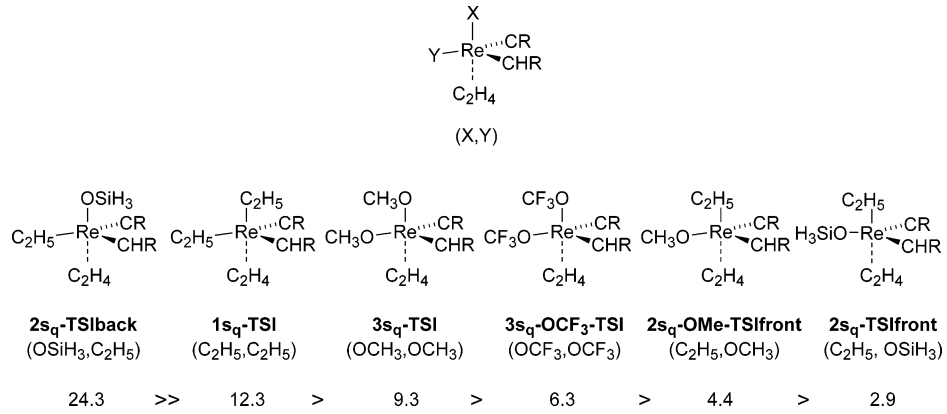

Table 3. Partitioning Energy Scheme (in kcal mol^{-1}) for the Energy Barrier of the Transition State for Ethylene Coordination and for the Ethylene Complex (see eq 2)

	1s$_q$[a]		2s$_q$[a]		2s$_q$-OMe[a]		3s$_q$[a]	
	TSI	II	TSI	II	TSI	II	TSI	II
ΔE	12.4	7.2	2.9	−0.2	4.4	1.4	9.3	−1.2
ΔE_{dis}(Re)[a]	13.1	25.6	3.5	11.5	5.3	12.9	9.9	21.8
ΔE_{dis}(ll)[a]	0.1	3.3	0.0	1.5	0.0	1.5	0.1	3.6
ΔE_{int}[a]	−0.8	−21.7	−0.6	−13.2	−0.9	−13.0	−0.7	−26.6

[a] See text for definition.

negligible. We will thus discuss the ranking of transition states exclusively based on the energy required to distort the tetrahedron to a trigonal prismatic geometry. In such a geometrical change, X becomes trans to an empty coordination site, and Y becomes coplanar with the alkylidyne and alkylidene ligands. The distortion energy is minimized when the best σ-donor ligand finds the most available metal orbital to maximize its bonding interaction (no ligand in trans, hence the apical site). Likewise, it is also minimized when a poor σ-donor ligand competes the least with the metal-alkylidyne and metal-alkylidene bonds, hence the basal site. This accounts for the effect of (X,Y) on the energy barriers (vide supra Scheme 6).

Furthermore, X and Y modify the geometries of the reactant ***n*s$_q$** (n = 1−3), so that the deformation to reach the corresponding transition states ***n*s$_q$-TSI** (n = 1−3) is altered. Thus the difference of the sum of the bond angles $\sum\alpha$ (Y−Re-alkylidyne, alkylidyne-Re-alkylidene, alkylidene-Re−Y) between the reactant ***n*s$_q$** (n = 1−3) and the transition state ***n*s$_q$-TSI** (n = 1−3) measures how much the Y-alkylidyne-alkylidene face is already open. The effect of (X,Y) on $\sum\alpha$ is as follows: it varies from 300.7 to 349.4 (Δ = 48.7°) for (OSiH$_3$, CH$_2$CH$_3$), 317.5 to 353.7° (Δ = 36.2°) for (CH$_2$CH$_3$, CH$_2$CH$_3$), 320.3 to 349.2° (Δ = 28.9°) for (OCH$_3$, OCH$_3$), 313.6 to 344.6° (Δ = 31°) for (OCF$_3$,OCF$_3$), 313.7 to 344.7° (Δ = 31°) for (CH$_2$CH$_3$, OCH$_3$), and 337.5 to 353.3° (Δ = 15.8°) for (X = CH$_2$CH$_3$, Y = OSiH$_3$). The X and Y ligands associated with the lower energy barrier also prepare the geometry of the catalyst to be close to that of the transition state for olefin coordination.

The transition states ***n*s$_q$-TSI** lead to ethylene adducts ***n*s$_q$-II**, having TBP geometries with an apical ethylene in which the Re-ethylene interaction is stronger, as shown by shorter Re−C distances (Tables 1, S1, and S2), and in which the alkylidyne, alkylidene and Y group are completely coplanar ($\sum\alpha$ = 360° for all complexes). Ligands with weaker trans influence (OCH$_3$ vs CH$_2$CH$_3$) allows a stronger Re-ethylene interaction, thus generating a relatively more stable adduct. As a consequence, **3s$_q$-II** is slightly more stable than **2s$_q$-II**. The energy partitioning of ΔE in these ethylene adduct **ns$_q$-II** shows a large distortion energy and a rather large interaction energy with the ethylene (Table 3). Therefore, the relative energies of the olefin adduct are not anymore determined by the distortion energies of the metal fragment.

Coupling Re=C and C=C: The Making of the Metallacyclobutane. From the ethylene adduct, the next step is the formation of the metallacyclobutane. In all cases, the metallacyclobutane found on the reaction pathway is a trigonal bipyramid with apical alkylidyne and Y groups and an essentially planar ring. Similar geometrical features have been found for the Mo-imido complexes.[26,28] The stability of the metallacyclobutanes with respect to the entry point increases with the increasing number of less donating ligands: **1s$_q$-III** (X = Y = CH$_2$CH$_3$; −1.0 kcal mol^{-1}) < **2s$_q$-OMe-III** (X = CH$_2$CH$_3$, Y = OCH$_3$; −9.6 kcal mol^{-1}) < **2s$_q$-III** (X = CH$_2$CH$_3$, Y = OSiH$_3$; −12.6 kcal mol^{-1}) < **3s$_q$-III** (X = Y = OCH$_3$; −15.2 kcal mol^{-1}) < **3s$_q$-OCF$_3$-III** (X = Y = OCF$_3$; −23.7 kcal mol^{-1}). The stability of the metallacyclobutanes relative to the reactants can be rationalized on the basis of trans influence, exerted by Y, which is trans to the alkylidyne. The metallacycle is increasingly stable as poorer σ-donor ligands are present: **1s$_q$-III** (X = Y = CH$_2$CH$_3$, −1.0 kcal mol^{-1}) < **2s$_q$-OMe-III** (X = CH$_2$CH$_3$, Y = OCH$_3$, −9.6 kcal mol^{-1}) < **2s$_q$-III** (X = CH$_2$CH$_3$, Y = OSiH$_3$, −12.6 kcal mol^{-1}).

The transition states **ns$_q$-TSII** connecting the ethylene adduct to the metallacycle have been located for (X = Y = CH$_2$CH$_3$) and for (X = CH$_2$CH$_3$, Y = OSiH$_3$ or OCH$_3$). In all complexes, the energy barrier is very small (energy barrier of less than 2 kcal mol^{-1}). In the case of the bis-alkoxy complex, no transition state could be located on the entry channel, which is consistent with a very small barrier. In fact, a tiny energy barrier of 0.4 kcal mol^{-1} above the propene adduct is obtained on the exit channel. Likewise, no transition state could be located for **3s$_q$-OCF$_3$-TSII** (X = Y = OCF$_3$). In the case of alkoxy or fluorinated alkoxy ancillary groups, one cannot exclude that the olefin adduct may not be a stable enough minimum to create a barrier for C−C coupling. Thus, the only transition state is that corresponding to the olefin coordination. Therefore, for these two alkoxy ligands, the key transition state for the reaction is that associated with the coordination of the olefin and not with the C−C coupling. It is an early transition state with respect to the C−C bond formation not because there is a change in early

vs late nature of the transition for the metallacyclobutane formation but because it is the transition state for the preceding elementary step on the reaction pathway.

Two factors lower the transition state: a stronger interaction between the Re═C and the C═C bond, and a Y ligand with a small trans influence as it becomes trans to the alkylidyne (vide supra). Both are favored by the presence of poor electron donating ligands. Additionally, a Natural Population Analysis (NPA) on the reactant shows that the Re═C polarization is the largest for the weaker σ-donor ligands and is as follows: **3s$_q$-OCF$_3$** (q(Re) = +1.12 and q(C) = −0.37) ≈ **3s$_q$** (q(Re) = +1.15 and q(C) = −0.40) > **2s$_q$** (q(Re) = +0.85 and q(C) = −0.34) > **1s$_q$** (q(Re) = +0.78 and q(C) = −0.34). As it was mentioned earlier,[37] the O-based group acts on the metal as overall an electron withdrawing group and increases the positive charge on the metal. This polarizes all metal ligand bonds and in particular the Re═C bond. The haptotropic shift of the ethylene from η^2 (in **ns$_q$-II**) to η^1 (in the **ns$_q$-TSII**) polarizes the C−C bond such as a positive charge develops on the carbon further away from the metal. This makes the carbon nearer the alkylidene more electrophilic and contributes to the lowering of the energy barrier for metallacycle formation.

Consequence on the Overall Catalytic Cycle. The reaction pathway for olefin metathesis with Re(≡CR)(═CHR)(X)(Y) has two independent individual steps with energy barriers very sensitive to the nature of X and Y as well as the nature of the substituents on the alkylidene and the olefin. The barrier for the first step is early with respect to the C−C bond formation between the olefin and the alkylidene, while the barrier for the second step is late with respect to the C−C formation. It should be noted that, for the two transition states, the metal fragment is distorted compared to a tetrahedral geometry so that the analysis in terms of early-late is not valid for the metal fragment. Our calculations show that the transition states for the [2+2] cycloreversion of the metallacyclobutane are higher than those for the [2+2] cycloaddition. Thus, a transition state has been located for the case (X = Y = OCH_3) on the exit channel but not on the entry channel. If the full substituents and ligands of the catalytic systems are included in the calculations, it should not be excluded that transition states could be located for the metallacycle formation and opening because of the increased steric hindrance as the metallacyclobutane is formed.

A good catalyst is associated with low activation barriers for all individual steps and not too low energy wells for all minima, in other words with a shallow (potential) free energy surface. The calculations of the free energies for the present reaction have shown that the entropy has an increasing effect in the order ***n*s$_q$−TSI** < olefin adduct ***n*s$_q$-II** < ***n*s$_q$-TSII**, metallacyclobutane, ***n*s$_q$-III**. Therefore, the change in free energy differences between the first transition state corresponding to the approach of the olefin and the metallacycle should be smaller than indicated by the difference in energies (compare Figures 5 and 6). However, a more quantitative evaluation of the entropic part is needed for a better estimation of the relative free energies of the two elementary steps. With the present way to calculate free energies, it is still uncertain which of the two steps is the rate-determining step.[40] However, the effect of X and Y on the relative *E* and *G* values of a given step is most likely to be properly calculated. We can thus relate the experimental observation to the calculated energy and free energy profiles. The order of reactivity of the molecular complexes is as follows Re(≡CR)(═CHR)(CH_2tBu)$_2$ < Re(≡CR)(═CHR)(OtBu)$_2$ < Re(≡CR)(═CHR)(OR_{6F})$_2$ (R = tBu, R_{6F} = C(CH_3)(CF_3)$_2$). This is accounted for by the lowering of the transition state for coordinating the olefin and by the lowering of the transition state for the [2+2] cycloaddition. No transition state for the [2+2] cycloaddition or cycloreversion could be located in our calculations with the OCF_3 model for partially fluorinated alkoxy groups used experimentally. Note that our calculations exaggerate the effects of the fluorinated alkoxy group since OCF_3 has been used in place of OC(CH_3)(CF_3)$_2$, and therefore the energies of all extrema probably lie between those of the OCF_3 and OCH_3 systems, most likely closer to the OCH_3 system. Moreover, the metallacyclobutane should not be in a deep well in term of free energy and also should be destabilized more than any other structure by the substituents on the alkylidyne, alkylidene, and olefin. This accounts for the increased reactivity when introducing poorer electron donor ancillary X and Y ligands. Finally, the calculations show that having an asymmetric system, that is, having Y as a siloxy or a methoxy ligand (poor σ-donor) and X as an alkyl (strong σ-donor) allows the first transition state to be lowered and the metallacyclobutane to be destabilized. This, in turn, decreases the difference between minima and maxima, and readily explains why the silica supported system Re(≡CtBu)(═CHtBu)(CH_2tBu)(OSi≡) is much more reactive than Re(≡CtBu)(═CHtBu)(OR_{6F})$_2$.

Conclusion

It has been often considered that the key steps of the olefin bond metathesis are the [2+2] cycloaddition between the C═C and M═C π bonds and the corresponding cycloreversion. This assumes that there is no barrier for the olefin to approach the electron deficient metal center. The calculations show that the olefin π-bond metathesis between ethylene and various Re(≡CR)(═CHR)(X)(Y) complexes starts with an elementary step that has a significant energy barrier. This step does not create any significant interaction between the C═C and Re═C π-bonds, but prepares the catalyst for the C−C coupling. During this preparation step, the pseudo-tetrahedral structure of the catalyst is modified to generate an empty coordination site to accommodate the incoming olefin. The energy barrier of the preparation step is optimized by having poor σ-donor ligands, experimentally the best ligands for homogeneous olefin metathesis catalysts, or better yet when the two ligands have different electronic properties: one ligand must be a good σ-donor and the other one must be a poor σ-donor, as observed for the silica supported system, Re(≡CtBu)(═CHtBu)(CH_2tBu)(OSi≡). The energy barrier for the second step, the [2+2] cycloaddtion, is low in all cases and is still favored by poor σ-donor ligands. Poor σ-donor ligands also stabilize the metallacyclobutane intermediates relative to the separated reactants. The best catalyst is the one associated with the most shallow potential or free energy surface. An olefin metathesis catalyst having a geometry very close to that of the transition state associated with the coordination of an olefin (low energy barrier), and generating a not too stable metallacyclobutane intermediate would be an efficient catalyst. Experimentally, it turns out that the most highly active catalyst is Re(≡CtBu)(═CHtBu)(CH_2tBu)(OSi≡), prepared by grafting Re(≡CtBu)(═CHtBu)(CH_2tBu)$_2$ on a silica surface, which bears two ligands with different electronic properties, a good (CH_2tBu) and a poor (OSi≡) σ-donor ligands.

These results show that the stable geometry of d^0 olefin metathesis catalyst (tetrahedron) may not be prepared to react with an incoming olefin. A related situation is found with Grubbs'type catalyst precursors, which must lose a phosphine ligand to become active. These two different families of efficient olefin metathesis catalysts have in fact a common feature: a protected coordination site, the Grubbs'type catalyst via an additional ligand and the Schrock's type via a spherical geometry. The rate determining step for d^0 systems is not *a fortiori* the coupling of the C═C and M═C π bonds, but the generation of a coordination site, as it has already been shown for the Grubbs'type catalysts. This could be key to the design of better catalysts.

Acknowledgment. X.S.M. thanks the CNRS for a postdoctoral position, the IDRIS (Grant No. 041744) and CINES (Grant No. lsd2217) french national computing centers for a generous donation of computer time.

Supporting Information Available: Tables S1 and S2 giving the selected geometrical parameters for the extrema located along the metathesis pathways of C_2H_4 with $Re(\equiv CCH_3)(=CHCH_3)(CH_2CH_3)(OSiH_3)$ and $Re(\equiv CCH_3)(=CHCH_3)(OCH_3)_2$ respectively. Figure S1 giving the optimized geometries of the extrema located along the metathesis pathway of C_2H_4 with *anti*-$Re(\equiv CCH_3)(=CHCH_3)(CH_2CH_3)$. Figure S2 optimized geometry for $\mathbf{1_q}$**-TSIbottom**. Full list of authors for ref 32. List of Cartesian coordinates, *E* and *G* absolute values (u.a.) of all extrema. This material is available free of charge via the Internet http://pubs.acs.org.

JA053528I